PAPER

Engineering stress in thin films for the field of bistable MEMS

IOP Publishing Journal of Micromechanics and Microengineering
J. Micromech. Microeng. **25** (2015) 125025 (7pp) doi:10.1088/0960-1317/25/12/125025

Engineering stress in thin films for the field of bistable MEMS

Dilan Ratnayake[1], Michael D Martin[2], Usha R Gowrishetty[1], Daniel A Porter[3], Thomas A Berfield[3], Shamus P McNamara[1] and Kevin M Walsh[1]

[1] Department of Electrical and Computer Engineering, University of Louisville, Louisville, KY, USA
[2] Department of Physics, University of Louisville, Louisville, KY, USA
[3] Department of Mechanical Engineering, University of Louisville, Louisville, KY, USA

E-mail: walsh@louisville.edu

Received 16 June 2015, revised 22 July 2015
Accepted for publication 3 August 2015
Published 11 November 2015

Abstract

While stress-free and tensile films are well-suited for released in-plane MEMS designs, compressive films are needed for released out-of-plane MEMS structures such as buckled beams and diaphragms. This study presents a characterization of stress on a variety of sputtered and plasma-enhanced chemical vapour deposition (PECVD)-deposited films, including titanium tungsten, invar, silicon nitride and amorphous silicon, appropriate for the field of bistable MEMS. Techniques and strategies are presented (including varying substrate bias, pressure, temperature, and frequency multiplexing) for tuning internal stress across the spectrum from highly compressive (-2300 MPa) to highly tensile (1500 MPa). Conditions for obtaining stress-free films are also presented in this work. Under certain conditions during the PECVD deposition of amorphous silicon, interesting 'micro-bubbles' formed within the deposited films. Strategies to mitigate their formation are presented, resulting in a dramatic improvement in surface roughness quality from 667 nm root mean square (RMS) to 16 nm RMS. All final deposited films successfully passed the traditional 'tape test' for adhesion.

Keywords: bistable, MEMS, engineered stress, buckle, PECVD, sputter

(Some figures may appear in colour only in the online journal)

1. Introduction

Bistable devices are all around us from the unique conical auditory hair bundles found in the human ear [1, 2] to the common mechanical wall switches found in homes for turning lights on and off. However, until very recently, bistable structures have not been implemented for miniature mechanical devices and systems. Over the last few years, bistable elements have started to be adopted by the MEMS (micro-electro-mechanical systems) community as they have the potential to serve as building blocks for a new generation of sensors and actuators. Bistable devices have some unique advantages over their linear non-bistable counterparts. They can be configured as 'threshold detection' devices for capturing critical events due to their inherent mechanical hysteresis. This also allows them to exhibit built-in 'non-electronic memory' for mechanically recording and storing of important events. If designed properly, they can even be configured as true no-electrical power (NEP) sensors and devices. Potential application areas for these novel bistable elements include mechanical switches [3], bistable vibration energy harvesters [4], micro-valves [5], micro-pumps [6], no-electrical-power sensors [7], and mechanical memory elements [8]. Several methods for fabricating bistable structures, such as buckled beams and diaphragms, have been reported in the literature along with proposed actuation methods including electrostatic [9], pneumatic [10], magnetic [11] and thermal means [12]. Our research group has been very active in this emerging field. In 2010 we developed a reliable fabrication process for producing buckled circular diaphragms using stress-engineered thermal oxide coupled with low-stress polyimide (PI) for structural enhancement and stability [13]. The cross-section of that device is illustrated in figure 1(a), along with its bistable deflection to applied pressure (figure 1(b)). In 2010, we used a similar process to fabricate a no-electrical power,

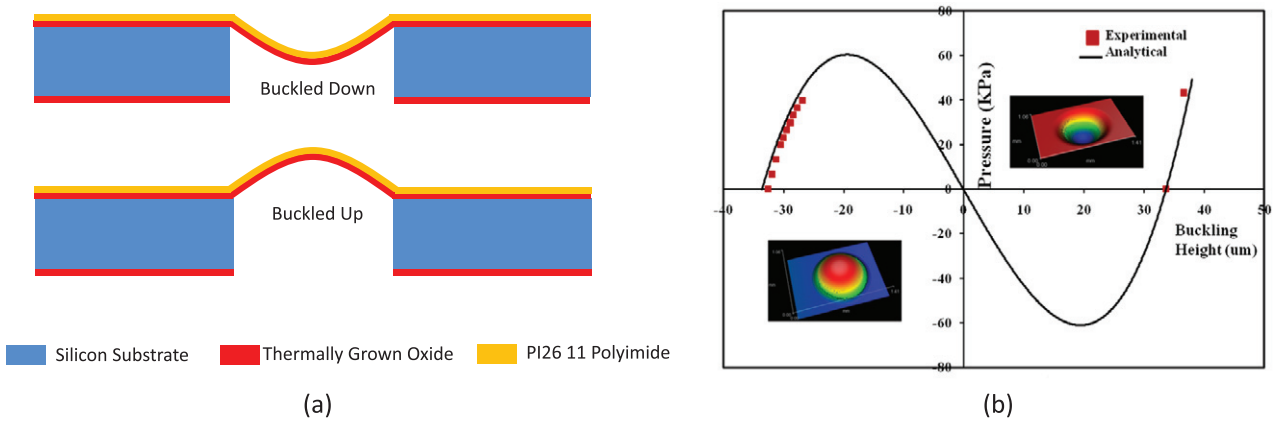

Figure 1. (a) Bistable MEMS diaphragms fabricated using thermal oxidation, polyimide spin coating, and deep reactive ion etching (DRIE). (b) Theory versus experimental diaphragm deflection to pressure demonstrating a snapping displacement of +/− 35 μm at the center of the 900 μm diameter buckled diaphragm [14] © 2010 IEEE. Reprinted, with permission, from Gowrishetty U R, Walsh K M and Jackson D 2015 No-power vacuum actuated bi-stable MEMS SPDT switch *IEEE Sensors* pp 1745–9.

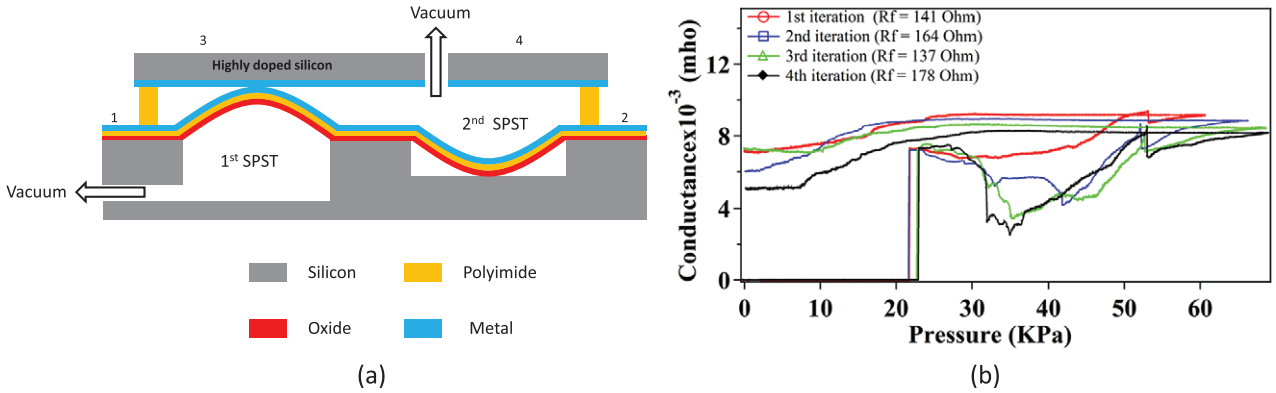

Figure 2. (a) Cross-section of the University of Louisville bistable, normally-open, vacuum-actuated, SPST MEMS switch. (b) Switch conductance versus pressure for four iterations of vacuum followed by applied pressure. Contact resistance of the switch was less than 200 ohms when closed [14] © 2010 IEEE. Reprinted, with permission, from Gowrishetty U R, Walsh K M and Jackson D 2015 No-power vacuum actuated bi-stable MEMS SPDT switch *IEEE Sensors* pp 1745–9.

bistable, pressure-actuated SPST (single pole single throw) MEMS switch as shown in figure 2(a) and demonstrated its performance under variations of applied vacuum and pressure (figure 2(b)) [14]. In 2012, we published a paper demonstrating how our PI/oxide buckled diaphragms could serve as the heart of an energy harvesting device [15]. In all of these examples, thermally grown silicon dioxide films were used as the principle source of the internal stress required for buckling. For the field of bistable MEMS to continue to evolve and expand, additional stress-engineered materials need to be developed. In this paper, we investigate other interesting candidate materials for engineering stress in thin films for potential use as bistable elements. Specifically, we report on using sputtering and PECVD (plasma-enhanced chemical vapor deposition) techniques for controlling stress in deposited silicon nitride, amorphous silicon, titanium tungsten, and invar thin films.

2. Experimental details and results

Since most MEMS devices are fabricated from layers of silicon combined with electrically conductive and insulating films, we selected the following materials to study: titanium tungsten, invar, silicon nitride and amorphous silicon. Titanium tungsten (TiW) was chosen because it is a good conductive layer and can also be used as an adhesion layer for other metals. Invar was selected because it can be utilized as an effective passive layer (i.e. low CTE) in thermally actuated MEMS devices. Silicon nitride was selected because it is a common MEMS insulating layer and it also serves as an excellent adhesion layer for amorphous silicon. Finally, amorphous silicon was selected because it is a common form of silicon deposited using PECVD and sputtering equipment, and used for thin film MEMS application for both its mechanical properties and, when doped, its electrical properties [16, 17]. In all of our experimental investigations, 100 mm diameter (1 0 0) *n*-type Si wafers (4–10 Ωcm) were used as the starting substrates. They were cleaned using the traditional industry-standard RCA1 and RCA2 cleaning procedures [18]. The initial wafer bow was measured using a laser-based Toho Thin Film Stress Measurement System (KLA Tencor FLX-2320, USA). Each wafer was measured at 4 different angles (0°, 45°, 90° and 135°) before any thin film deposition. Then the candidate films were deposited onto the top surface of the wafers and the bow measurements were repeated. From those data, the internal biaxial stresses of the deposited thin films were calculated using the supplied Toho software which is based upon the Stoney equation [19]. The

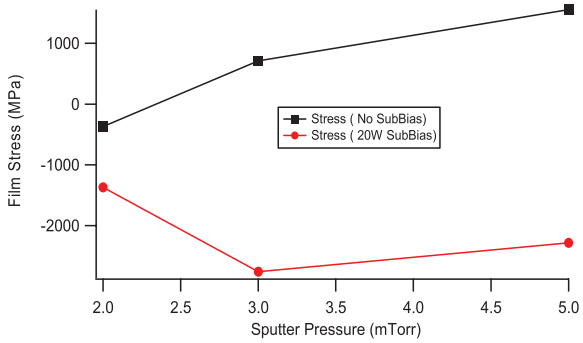

Figure 3. Stress in sputtered TiW thin films with and without substrate bias. All samples were deposited at 300 W DC for 20 min, which resulted in film thicknesses of 160 ± 5 nm.

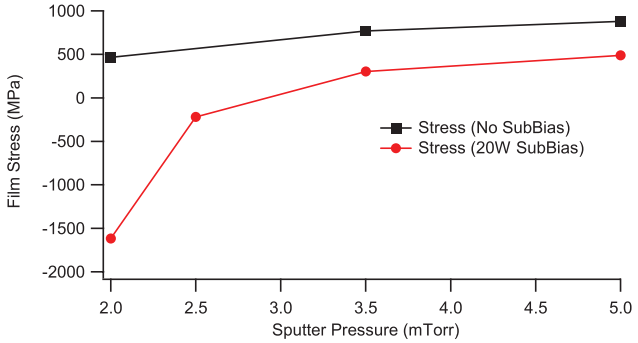

Figure 4. Stress in sputtered invar thin films with and without substrate bias. All samples were deposited at 300 W DC for 20 minutes, which resulted in a film thickness of 140 ± 5 nm for all data points.

thickness of the candidate films were measured using either a Dektak Profilometer or a Filmetrics Thin Film Measurement System. A shadow mask was used to create a step when depositing the thin films for the Dektak Profilometer measurements. The thickness is then used as part of the calculation to determine the stress. However, separate samples were used to evaluate film thickness as the stress calculation requires uniform un-patterned films. Typical film thicknesses are stated for each set of experiments.

2.1. Titanium tungsten films

It is well known that the thin film stress of sputtered metal layers can be tuned by adjusting the kinetic energy of arriving neutral metal atoms so that at lower sputter pressures (and higher kinetic energy) the film becomes more compressive [20, 21]. Essentially, the film becomes denser and contains fewer voids at lower sputter pressures. A similar effect can be achieved by providing a small substrate bias (either RF or DC) during the deposition so that Ar ions bombard the substrate (not the target) with sufficient energy to allow metal atoms and clusters to 'walk' on the surface until surface defects are found to fill. In particular, the intrinsic film stress of TiW is known to be readily adjustable from roughly +1000 MPa tensile to −2000 MPa compressive by changing the Ar pressure during sputter deposition from 2 mTorr to 20 mTorr [21].

In this work, sputtering was used to deposit the thin-films of TiW from a 4' diameter target composed of 10% Ti and 90% W. Sputtering was performed with a PVD 75 RF/DC Sputtering System from Kurt J. Lesker. For all experiments the power was 300 W DC and the deposition time was 20 min while the pressures were varied and this produces 160 ± 5 nm thick film.n some experiments a capacitively coupled RF substrate bias was used at 20 W which produced a DC bias of 277 V at 3 mTorr, 270 V at 5 mTorr and 107 V at 2 mTorr due to poor coupling. Figure 3 shows our results with and without substrate bias. With no bias, we were able to vary the film's stress from approximately −300 MPa to +1500 MPa consistent with findings in the literature. However, with bias we could further control stress from −1300 MPa to −2300 MPa. The addition of the substrate bias allowed compressive stresses to be tuned into the films, which is the basic requirement for thin film buckling when released. To our knowledge, this is the first time a stress characterization curve for TiW has been published with a substrate bias. In general this method allows one to adjust film stress at relatively higher pressures thus enabling deposition of compressive TiW films at higher deposition rates. Additionally, many capacitively coupled sputtering systems are not capable of sustaining plasmas at such low pressures (<5 mTorr) therefore substrate biasing allows the manipulation of TiW film stress at less challenging pressures.

2.2. Invar films

Invar was developed by the French physicist Charles Guillaume in 1897 [22] and consists of an alloy with the composition of 36% Ni and 64% Fe. The advantage of this ferromagnetic face-centered cubic alloy is that it has a very small and invariant coefficient of thermal expansion (CTE) in the temperature range between −100 °C and +160 °C, thus the reason for its name [22]. In this research a 4' invar sputtering target was purchased and the invar thin film was deposited on a 100 mm diameter (1 0 0) Si wafer using the same Kurt Lesker PVD 75 RF/DC sputtering system as discussed above. The same procedure that was used to deposit TiW thin film was used to deposit sputtered Invar thin films. For all experiments the power was 300 W DC and the deposition time was 20 min while the pressures were varied from 2 to 5 mTorr, these processing conditions provide 140 ± 5 nm thick film. In some experiments a capacitively coupled RF substrate bias was used at 20 W which produced an average DC bias of 280 V to produce a denser film. As shown in figure 4, application of a 20 W substrate bias resulted in more film stress variation with chamber pressure. Without substrate bias, it was not possible to tune compressive stress into the films. This combination of deposition with and without bias allows one to create invar films ranging from −1600 MPa to +300 MPa, providing much latitude with the MEMS design of bistable and non-bistable structures.

2.3. Silicon nitride films

An Oxford PECVD System 100 using silane and ammonia was used to deposit silicon nitride films. The films were

Table 1. Process settings for PECVD SiN_x deposition.

	Parameters								
Material	SiH4 5% in Ar (sccm)	NH3 (sccm)	N2 (sccm)	LF Power (W)	HF Power (W)	Pressure (mTorr)	Time (min)	Temperature (°C)	Thickness (nm)
SiN_x	20	20	600	20	20	650	15	400	130–140

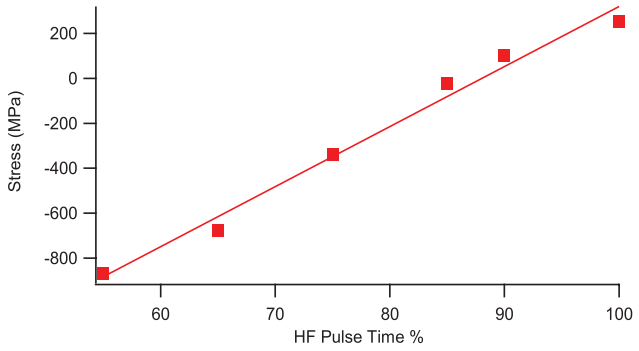

Figure 5. SiN_x film stress versus HF pulse percentage. (15 min, 400 °C, 135 ± 5 nm film thickness, 20 s pulse time, 20 W LF at 100–350 kHz, 20 W HF at 13.56 MHz, 650 mTorr pressure, 20 sccm 5% SiH_4 in Ar, 20 sccm NH_3, 600 sccm N_2).

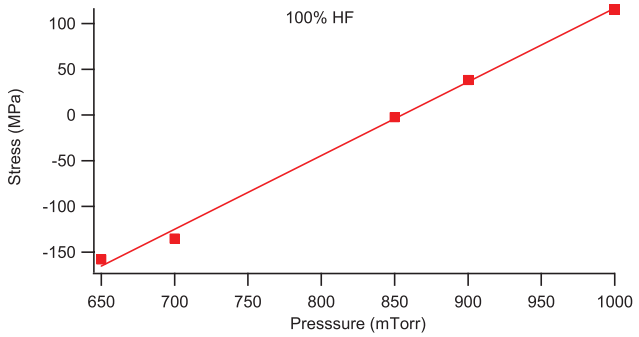

Figure 6. Stress on SiN_x film versus pressure with 100% HF. (15 min, 400 °C, constant 20 W HF at 13.56 MHz, 20 sccm 5% SiH_4 in Ar, 20 sccm NH_3, 600 sccm N_2, film thicknesses of 344, 363, 475, 507, and 604 nm from left to right data points).

deposited onto a 100 mm silicon (1 0 0) wafers as before. The details of the process settings are presented in table 1.

The stress on the nitride films were controlled by changing the high frequency (HF) pulse time in dual frequency mode as described in equation (1).

$$\text{HF Pulse } \% = \frac{\text{HF Pulse Time}}{(\text{LF Pulse Time}+\text{HF Pulse Time})}100\% \quad (1)$$

where HF refers to high frequency (13.56 MHz) and LF refers to low frequency (100–350 kHz) power. Figure 5 shows the stress on the SiN_x film verses HF pulse percentage. As seen in the figure, it is possible to produce a near stress-free film (i.e. less than −20 MPa) using an 85% HF pulse recipe. Note that this recipe will be used in the next section for producing a thin stress-free adhesion layer of silicon nitride which is needed for PECVD-deposited amorphous silicon.

A second experiment was performed to observe how deposition pressure effects the stress on the nitride film. In this series of experiments, the high frequency was operated continuously (i.e. HP Pulse % = 100%). Figure 6 presents the results illustrating a very linear dependence of silicon nitride film stress on chamber pressure, with the interesting ability to tune the internal stress of the deposited films from tensile to stress-free to compressive. The results in this section illustrate how the internal stress of PECVD-deposited silicon nitride films can be readily adjusted using either HF % or chamber pressure. While these results have never been published for our deposition tool, similar results exist for other PECVD equipment. However, we needed to perform these experiments in order to determine how to deposit stress-free PECVD silicon nitride as a base for depositing amopous silicon, as discribed in the next section. Whereas the thicknesses of previous deposited films varied very little with process variations in the prior experiements, in this experiement pressure had a larger effect. As expected, deposition rates increased with pressure resulting in final thicknesses of 344, 363, 475, 507, and 604 nm SiN_x films for 650, 700, 850, 900 and 1000 mTorr of pressure respectively.

2.4. Amorphous silicon films

Amorphous silicon (α-Si) is a popular deposition material for MEMS and very little has been published regarding methods to effectively tune its internal stress properties for various non-traditional MEMS applications. For our experiment, undoped amorphous silicon was selected and deposited using PECVD. Specifically, the film's stress variation versus deposition temperature was investigated. Since amorphous silicon is known to show poor adhesion to bare silicon, it is traditionally deposited onto a SiO_x or SiN_x underlayer to improve adhesion [23, 24]. We did explore the possibility of depositing amorphous silicon directly onto bare silicon, but that resulted in very weak adhesion and the formation of 'micro bubbles' in the deposited films (see next section for images and further discussion). To overcome that problem, a stress-free film of silicon nitride was first deposited on the silicon substrates using the parameters extracted from the previous section. Then amorphous silicon films were deposited using the same PECVD system. The deposition temperature was varied from 150 °C to 300 °C. A summary of the deposition parameters are shown in table 2. The stress on the film was measured and the results for the undoped amorphous PECVD silicon are displayed in figure 7. Interestingly, we were able to obtain a nice linear range for internal stress versus deposition temperature, ranging again from tensile to compressive films. Near zero-stress α-Si films were obtained at a deposition temperature of 225 °C (average tensile stress was ~3.33 MPa). The compressive films are excellent candidates for buckled bistable MEMS structures. Deposition temperature played a role in the film's

Table 2. Process settings for PECVD α-Si deposition.

	Parameters					
Material	SiH4 5% in Ar (sccm)	HF Power (W)	Pressure (mTorr)	Time (min)	Temperature (°C)	Thickness (nm)
α-Si	25	7	1000	30	150–300	600–943

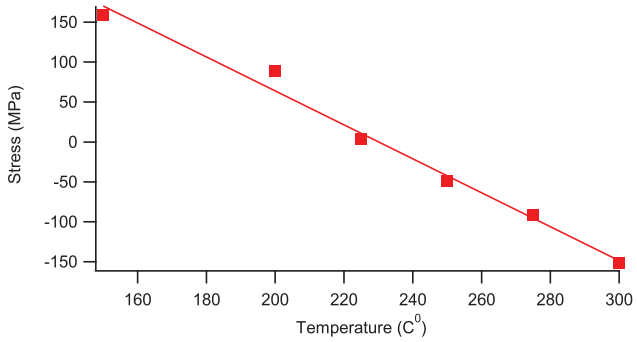

Figure 7. Stress on α-Si film versus temperature. (30 min, 7 W at 13.56 MHz, 1000 mTorr, 25 sccm 5% SiH_4 in Ar, film thicknesses of 600, 683, 688, 725, 728, and 943 nm from left to right data points).

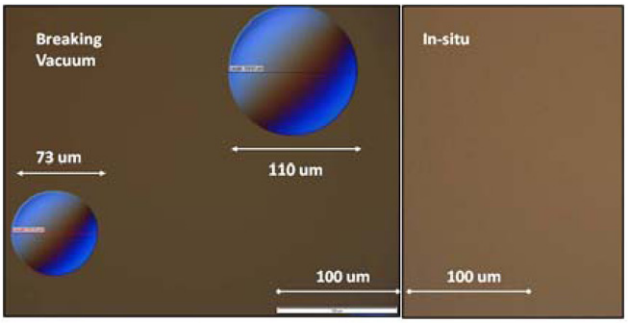

Figure 8. Optical image of PECVD amorphous silicon film deposited by breaking vacuum after the SiN_x deposition step (left) and without breaking vacuum (*in situ*, right).

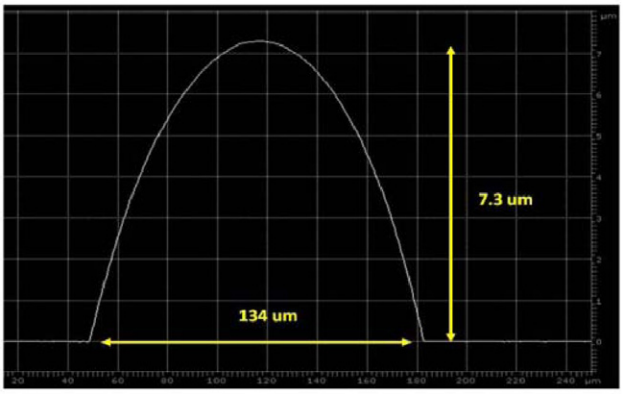

Figure 9. DEKTAK profile of one of the larger PECVD amorphous silicon micro-bubbles deposited on low-stress nitride. Diameter = 134 μm, height = 7.3 μm.

final thickness. The deposition rate increased with temperature, as expected, resulting in thicknesses of 600, 683, 688, 725, 728, and 943 nm for the data points in figure 7 proceeding left to right in the graph.

3. Discussion

As stated in the previous section, during the amorphous silicon study, some issues surfaced with the quality of the films when PECVD α-Si was deposited directly onto bare silicon. Specifically two problems were encountered. The deposited films demonstrated poor adhesion to the substrates and failed the traditional 'tape test' [25–28]. When a strip of adhesive tape was pulled from the film, it delaminated from the substrate. The second problem was with its morphology, as the film contained a large density of raised hallow 'micro-bubbles' ranging in diameter from 10 μm to 70 μm. The formation of such bubbles has been previously reported in the literature and has been attributed to trapped hydrogen gas unable to escape [29–31]. It is logical to think that both problems are somewhat related, as poor adhesion can provide regions on the surface for hydrogen to accumulate. To eliminate this problem, a thin layer of stress-free silicon nitride was deposited prior to the amorphous silicon. This eliminated the formation of the hallow micro-bubbles as long as the nitride and α-Si deposition were done *in situ* (without breaking vacuum). When the α-Si was deposited after breaking vacuum (which we initially had to do to verify that the nitride film was indeed stress-free using the Toho Measurement System), the micro-bubbles reappeared when the compressive stress of the α-Si exceeded -90 MPa ($\geqslant$275 °C deposition temperature). This was attributed once again to poor adhesion between the compressive α-Si film and the nitride film which had been exposed to atmosphere. Exposure to atmosphere can result in a partial oxidation of the thin film and the accumulation of adsorbed moisture leading to the generation of release hydrogen atoms when heated which combine at the weak interface generating trapped hydrogen bubbles as described above. To test this hypothesis, the same experiment was repeated without breaking vacuum between the nitride and α-Si depositions (i.e. *in situ*). The adhesion between the two films improved tremendously and the hallow micro-bubbles disappeared. Also supporting our hypothesis was the fact that the *in situ* deposition passed the traditional 'tape test', while the film deposited while breaking vacuum failed. A comparison of the two films is shown in figure 8 using DIC optical microscopy (500x). The left side of the figure shows representative micro-bubbles obtained when breaking vacuum between depositions. The right side presents results when performed *in situ*. The micro-bubbles ranged in diameter from 60 μm to 140 μm with typical heights of 3 μm to 7.5 μm. The density of the micro-bubbles was approximately 5 bubbles/mm^{-2}. The average roughness of the two surfaces, as measured by an AFM, was 16 nm RMS for the *in situ* film and 667 nm RMS when breaking vacuum. Figure 9 presents a Dektak image of a typical hallow micro-bubble with

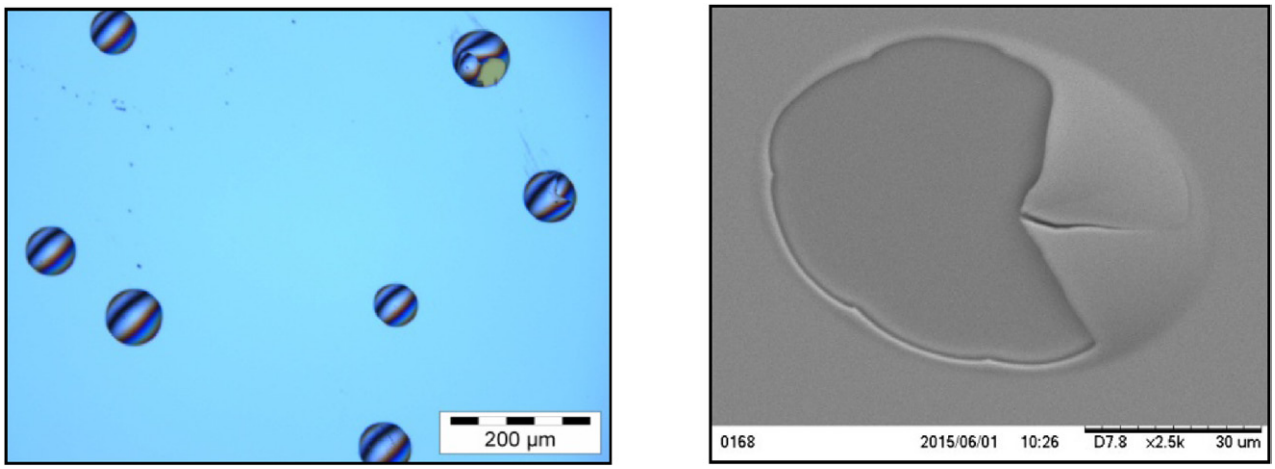

Figure 10. Optical image of amorphous silicon micro-bubbles which were PECVD deposited on low stress silicon nitride after breaking vacuum. Notice the two fractured bubbles in upper left corner of the image exposing underlying nitride layer (left), and SEM of a fractured micro-bubble (right).

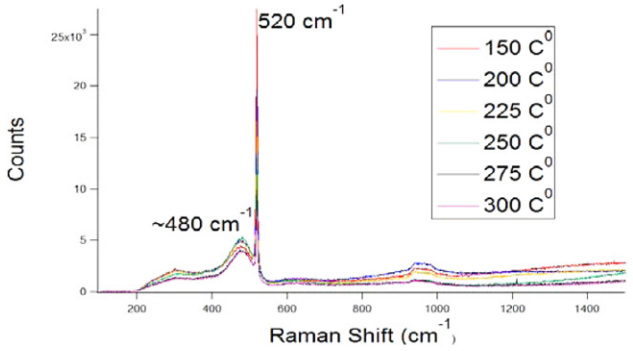

Figure 11. Raman spectra of PECVD amorphous silicon films versus deposited temperature. The sharp peak at 520 cm^{-1} is due to the silicon wafer substrate. The broad peak around 480 cm^{-1} is due to the amorphous PECVD silicon films.

a diameter of 134 microns and a height of 7.3 microns. If a controllable process could be developed for the formation of these interesting 3D structures, they could be used to fabricate bistable elements. To prove that the micro-bubbles were in fact hallow and not an accumulation of excess amorphous silicon as claimed in [23], some of them were intentionally fractured with a probe tip and imaged optically and using an SEM. These results are shown in figure 10 and illustrate that they are hallow.

Raman spectroscopy was used to verify that the films were indeed amorphous as shown in figure 11. The sharp peak at 520 cm^{-1} is due to the silicon wafer substrate and the broad peak around 480 cm^{-1} is an indication of the amorphous PECVD silicon films [32].

4. Conclusion

In summary, this paper reports on various deposition techniques for engineering the internal stress in candidate thin film materials for producing buckled bistable MEMS structures. Sputtering with and without substrate bias provided a new and excellent deposition technique for titanium tungsten and Invar. In both cases, the addition of a substrate bias provided a convenient means to greatly increase the compressive stress in the films, which is desirable characteristic when fabricating mechanically bistable elements. These are new findings previously unreported in the literature. For controlling the internal stress of amorphous silicon and silicon nitride, PECVD deposition was explored. With amorphous silicon, it was demonstrated that the stress could be controlled by varying the substrate temperature. With silicon nitride, the stress was controlled by either varying the HF/LF duty cycle or by varying the chamber pressure. Both strategies allowed for a full range of stress values to be obtained in the thin films—ranging from tensile to stress-free to compressive. This study introduces new strategies for intentionally engineering high levels of compressive stress into candidate films for released MEMS bistable devices.

Acknowledgments

This research was partially funded by NSF EPSCoR Award 0814194 and NSF Award 1408005 through the ECCS Division. The authors also wish to acknowledge the University of Louisville MicroNanoTechnology Center (MNTC) and its cleanroom staff lead by Dr Julia Aebersold for their assistance with the many fabrication processes.

References

[1] Gi-Woo K and Jaehwan K 2013 Compliant bistable mechanism for low frequency vibration energy harvester inspired by auditory hair bundle structures *Smart Mater. Struct.* **22** 014005

[2] 2009 The smallest chemical reaction system with bistability *BMC Syst. Biol.* **3** 90

[3] Huff M A, Nikolich A D and Schmidt M A 1991 A threshold pressure switch utilizing plastic deformation of silicon *Int. Conf. on Solid-State Sensors and Actuators, 1991. Digest of Technical Papers, TRANSDUCERS* pp 177–80

[4] Ando B, Baglio S, L'Episcopo G and Trigona C 2012 Investigation on mechanically bistable mems devices for energy harvesting from vibrations *J. Microelectromech. Syst.* **21** 779–90

[5] Popescu D S, Dascalu D C, Elwenspoek M and Lammerink T 1995 Silicon active microvalves using buckled membranes for actuation *8th International Conference on Solid-State Sensors and Actuators, 1995 and Eurosensors IX. Transducers* pp 305–8
[6] Nisar A, Afzulpurkar N, Mahaisavariya B and Tuantranont A 2008 MEMS-based micropumps in drug delivery and biomedical applications *Sensors Actuators* B **130** 917–42
[7] Hansen B J, Carron C J, Hawkins A R and Schultz S M 2007 Zero-power shock sensors using bistable compliant mechanisms *Proc. SPIE* **6525** 65251W
[8] Halg B 1990 On a micro-electro-mechanical nonvolatile memory cell *IEEE Trans. Electron Devices* **37** 2230–6
[9] Chan E, Garikipati K and Dutton R 1999 Complete characterization of electrostatically-actuated beams including effects of multiple discontinuities and buckling *Int. Conf. on Modeling and Simulation of Microsystems* pp 194–7
[10] Lisec T, Hoerschelmann S, Quenzer H, Wagner B and Benecke W 1994 Thermally driven microvalve with buckling behaviour for pneumatic applications *Proc. IEEE Workshop on Micro Electro Mechanical Systems, 1994 (IEEE)* pp 13–7
[11] Zhu Y and Zu J W 2013 Enhanced buckled-beam piezoelectric energy harvesting using midpoint magnetic force *Appl. Phys. Lett.* **103** 041905
[12] McCarthy M, Tiliakos N, Modi V, Frechette L G, International Mechanical Engineering C and Exposition 2007 Thermal buckling of eccentric microfabricated nickel beams as temperature regulated nonlinear actuators for flow control *Sensors Actuators* A **134** 37–46
[13] Gowrishetty U R, Walsh K M and Berfield T A 2010 Fabrication of polyimide bi-stable diaphragms using oxide compressive stresses for the field of 'Buckle MEMS' *J Micromech. Microeng.* **20**
[14] Gowrishetty U R, Walsh K M and Jackson D 2010 No-power vacuum actuated bi-stable MEMS SPDT switch *IEEE Sensors* pp 1745–9
[15] Porter D A, Gowrishetty U R, Phelps I J, Walsh K M and Berfield T A 2012 Mechanics of buckled structure mems for actuation and energy harvesting applications *ASME 2012 Int. Mechanical Engineering Congress and Exposition*: *(American Society of Mechanical Engineers)* pp 49–54
[16] Lim H C, Schulkin B, Pulickal M, Liu S, Petrova R, Thomas G, Wagner S, Sidhu K and Federici J F 2005 Flexible membrane pressure sensor *Sensors Actuators* A **119** 332–5
[17] Chang S and Sivoththaman S 2006 Development of a low temperature MEMS process with a PECVD amorphous silicon structural layer *J. Micromech. Microeng.* **16** 1307
[18] Kern W 1990 The evolution of silicon wafer cleaning technology *J. Electrochem. Soc.* **137** 1887–92
[19] Feng X, Huang Y and Rosakis A 2007 On the Stoney formula for a thin film/substrate system with nonuniform substrate thickness *J. Appl. Mech.* **74** 1276–81
[20] Maissel L I G R 1970 *Handbook of Thin Film Technology* (New York: McGraw-Hill)
[21] O'Donnell J K and Post R S 2002 Controlling stress in thin films (http://flipchips.com/tutorial/process/controlling-stress-in-thin-films/)
[22] Ucke C and Schlichting H 2009 Revival of the jumping disc *Phys. Ed.* **44** 612
[23] Chen-Kuei C, Ming-Qun T, Po-Hao T and Chiapyng L 2005 Fabrication and characterization of amorphous Si films by PECVD for MEMS *J. Micromech. Microeng.* **15** 136–42
[24] Xu Y, Fei F, Jin Z and Yuelin W 2009 Smooth surface morphology of hydrogenated amorphous silicon film prepared by plasma enhanced chemical vapor deposition *Plasma Sci. Technol.* **11** 569
[25] ASTM International 2009 *Standard Test Methods for Measuring Adhesion by Tape Test* (West Conshohocken, PA.: ASTM International)
[26] Ansi 2010 *Standard Test Method for Peel Adhesion of Pressure-Sensitive Tape* (Philadelphia, PA: ASTM International)
[27] Ohring M 1991 *The Materials Science of Thin Films* (Boston, MA: Academic)
[28] Volinsky A A, Moody N R and Gerberich W W 2002 Interfacial toughness measurements for thin films on substrates *Acta Mater.* **50** 441–66
[29] Shanks H and Ley L 1981 Formation of pin holes in hydrogenated amorphous silicon at high temperatures and the yield strength of a-Si: H *J. Appl. Phys.* **52** 811–3
[30] Mishima Y and Yagishita T 1988 Investigation of the bubble formation mechanism in a-Si: H films by fourier-transform infrared microspectroscopy *J. Appl. Phys.* **64** 3972–4
[31] Fu Y, Luo J, Milne S, Flewitt A and Milne W 2005 Residual stress in amorphous and nanocrystalline Si films prepared by PECVD with hydrogen dilution *Mater. Sci. Eng.* B **124** 132–7
[32] Deschaines T, Hodkiewicz J and Henson P 2009 Characterization of amorphous and microcrystalline silicon using Raman spectroscopy (Madison, WI: Thermo Fisher Scientific)